



Test Infrastructure and Accelerator Research Area

Status Report

Specification of emittance knobs

Aiba, M. (PSI) *et al*

30 May 2012

The research leading to these results has received funding from the European Commission under the FP7-INFRASTRUCTURES-2010-1/INFRA-2010-2.2.11 project TIARA (CNI-PP). Grant agreement no 261905.

This work is part of TIARA Work Package **6: SVET R&D Infrastructure**.

The electronic version of this TIARA Publication is available via the *TIARA web site* at <http://www.eu-tiara.eu/database> or on the *CERN Document Server* at the following URL: <http://cdsweb.cern.ch/search?p=TIARA-REP-WP6-2012-008>

Specification of emittance knobs

Masamitsu Aiba, Michael Böge, Natalia Milas, Andreas Streun, PSI Villigen, Switzerland;
Simone Liuzzo, INFN-LNF, Frascati, Italy.

May 14, 2012.

1 Introduction

The main objective of the work package SLS Vertical Emittance Tuning (SVET) is to upgrade the SLS storage ring to enable R&D on ultra-low vertical emittances. The existing instrumentation and its limitations had been described in previous reports [1, 2]: main upgrade project of SVET is the installation and commissioning of a high resolution beam size monitor in order to become able to verify emittances below 1 pm·rad.

This report will describe the methods for vertical emittance minimization which have been developed and applied up to now using the existing equipment. It thus mainly concludes the activities of task 6.2.2 “Specification of correction knobs and feedback algorithms for an automated correction of coupling, and algorithms for BBGA (beam-based girder alignment).”

Before applying methods for low emittance tuning, standard procedures for correction of machine imperfections have to be accomplished, which will not be described in this report. These procedures include orbit correction and fast orbit feedback [1, 3], correction of linear optics [2, 4] and determination of BPM roll errors [5]. Minor corrections of non-linear optics (i.e. tuning sextupole Hamiltonian modes [6]) interfere little with coupling correction and thus can be treated independently.

2 Beam-assisted girder alignment

As described in [1], the 49 girders of the SLS storage ring (12×4 girders numbered 1-48 for the 12 TBA arcs and girder 49 for the triplet of the FEMTO insertion [9]) can be moved in five degrees of freedom (three rotations and transverse displacements). The original proposal of a true beam-based girder alignment (BBGA), i.e. using deliberate girder misalignments as pseudo-correctors to center the orbit [10], had been rejected, since a) the girder “correctors” would also try to compensate for effects not related to their misalignments and result in non-realistic girder excursions, b) the procedure of girder movement contains some risk and thus requires great care, and c) source points for the user beam lines would be shifted.

Instead the girders were remotely realigned based on quadrupole survey data. The realignment

was performed with stored beam and running fast orbit feedback to verify successful moves by observing the decrease in corrector strengths. This procedure was named beam-assisted girder alignment (BAGA). Intermediate results had been reported in [2]. Meanwhile defective girder movers have been repaired and a complete BAGA procedure was accomplished.

With respect to vertical emittance minimization, the aim of BAGA is to eliminate sources of vertical dispersion η_y , which are due to relative vertical displacements of adjacent girders. After analyzing the vertical corrector pattern, girder-to-girder misalignments in the arc centers at the location of the central dipoles BX_i were identified to be the major source of η_y . The spatial corrector pattern analysis requires a Singular Value Decomposition (SVD) based orbit correction scheme utilizing a large number of (preferably all) eigenvalues in order to localize the girder-to-girder distortions [5, 7, 8].

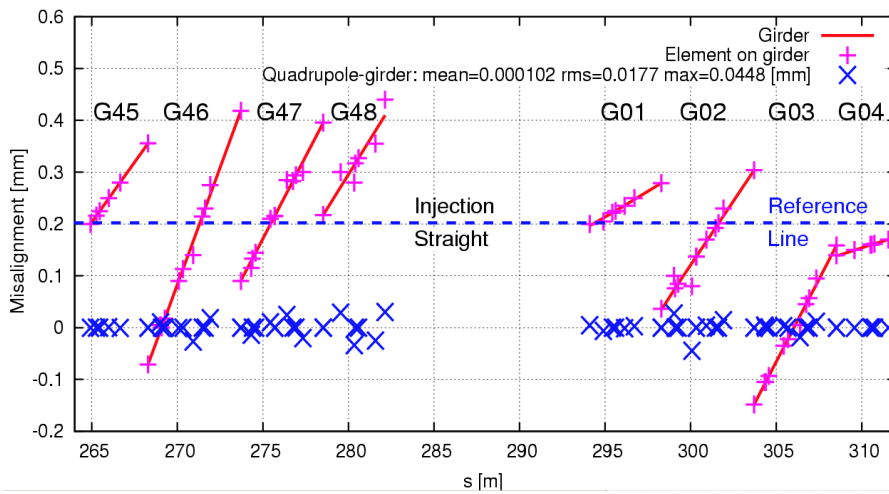


Figure 1: Quadrupole misalignments (+) in the sectors left and right of the injection straight. The lines are the corresponding girder fits for eight girders (G45-48, G01-04). The deviation of the individual quadrupole errors from the fit (x) shows an rms of $\approx 18 \mu\text{m}$. The alignment measurement error amounts to $\approx 10 \mu\text{m}$ over a distance of 2 m.

Analysis of vertical misalignment data taken for all quadrupoles in 2010 revealed that the corrector settings are closely correlated to the measured quadrupole positions. Furthermore the misalignments of the 177 quadrupoles are highly correlated since they are grouped on 49 girders which are the main source of the misalignments. As an example Fig. 1 depicts the quadrupole misalignments in the sectors adjacent to the injection straight. The deviation of the individual quadrupole errors from the fit to the girders features an rms value of only $\approx 18 \mu\text{m}$ which is ≈ 10 times smaller than the fitted rms girder misalignments.

Fig. 2 summarizes the necessary pitch (vertical angle) and heave (vertical position) changes for all girders. Since the suggested heave corrections exceed 0.6 mm a reference line has been defined by the fit of a smooth function to the corrections. The realignment of the girders to this non-zero reference line does not affect the machine performance due to its long spatial wavelength.

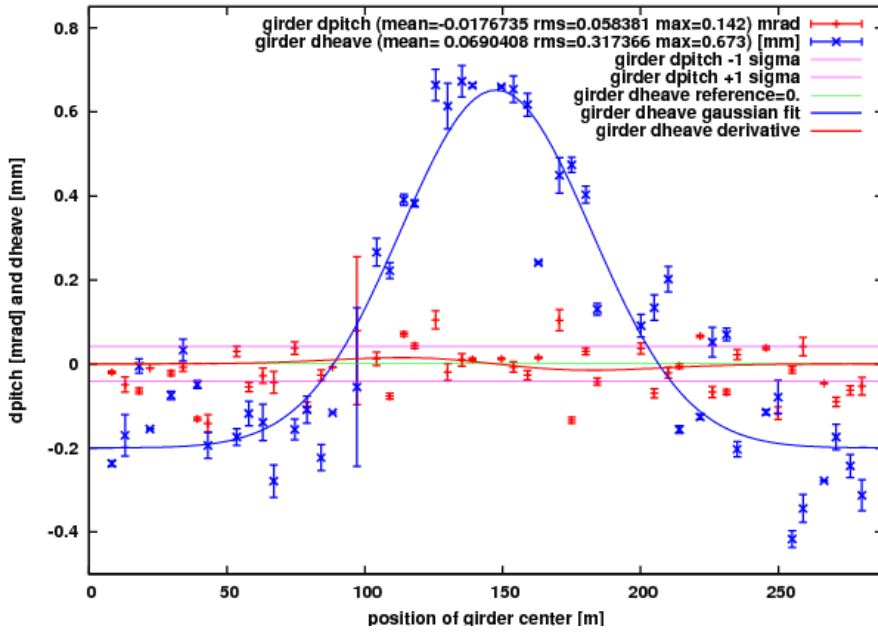


Figure 2: Pitch (+) and heave changes (×) for all girders based on the quadrupole misalignment survey data taken in 2010.

In April 2011 the realignment campaign was launched based on the 2010 survey data. Until the end of November all girders were successfully realigned. The realignment was merely done with stored beam and running fast orbit feedback [3] since the girders are remotely controlled [10] and the orbit effects of the proposed girder movements can be dynamically handled by the orbit correction system. This procedure allows a very precise control of the realignment process since the corrector variations within the feedback loop directly reflect the girder manipulations.

Since the 17 m long arc vacuum chambers, each extending over four girders which form one of the 12 sectors, can not follow the movement completely due to their stiffness, the BPM buttons, which are parts of the vacuum chambers, unavoidably move relative to the magnets. So a successive beam-based alignment (BBA) was performed to recalibrate the BPM centers relative to adjacent quadrupoles and lead to a further reduction of the vertical corrector strengths. An example for one sector had been given in the previous report [2]. A complete BAGA of the storage ring reduced the rms vertical corrector kick from ≈ 130 to ≈ 50 μrad rms. The distribution of kick strengths, which was non-Gaussian with highly populated tails before, became truly Gaussian after BAGA.

The reduction of corrector strength would allow to narrow the current range of the corrector power supplies in order to increase the resolution from present 1.4 nrad (corresponding to 1 ppm from the 20 bit ADCs [11] for a kick range of ± 740 μrad) to ≈ 0.5 nrad.

Subsequent correction of vertical dispersion η_y (see next section) achieved a value of 1.3 mm rms at only half the dispersive skew quadrupole strengths with respect to the situation before BAGA.

3 Model dependent correction methods

These methods rely on a beam dynamics model representing the real machine. They are expressed as a linear system of equations $\vec{m} = \mathcal{S} \cdot \vec{k}$ predicting a vector \vec{m} of measurements from a vector \vec{k} of knobs using a sensitivity matrix \mathcal{S} . Orbit correction is the classical example: model parameters (the knobs, e.g. corrector strengths) are fitted (e.g. by SVD “inversion” of the orbit response matrix) to reproduce measured data (e.g. BPM readings), and the inverse of the calculated changes of the parameters then is applied to the machine in order to shift the data towards some target values (e.g. reference orbit). Nonlinearities (e.g. BPM nonlinearities, sextupoles) may require several iterations.

The strength of these methods is the high correlation of the measurements through the model, which enforces physically sensible solutions and provides precise predictions and fast convergence. Eventually, the corrections are limited by model deficiencies and by measurement noise.

Two methods have been applied in SVET for coupling suppression:

3.1 VRM (vertical dispersion and response matrix)

The SLS storage ring has 36 skew quadrupoles, 12 located in dispersive regions and 24 in non-dispersive regions (in the standard optics labeled F6CW0). Vertical emittance is reduced by minimization of vertical dispersion using the 12 dispersive skew quads, and by minimization of betatron coupling using the 24 non-dispersive skew quads. These two steps are alternated and iterated. This method was the first one to be applied, starting already in times of SLS commissioning with a smaller number of skew quadrupoles, and was upgraded continuously. It has been previously described [2, 7], and is summarized here for completeness:

The settings for 12 dispersive ($\eta_x \approx 0.3$ m) skew quadrupoles are determined by applying the SVD “inverted” (no weighting factor cut) model-based 73×12 sensitivity matrix $\partial\eta_{yi}/\partial k_j$ to the measured spurious vertical dispersion η_y . (η_{yi} denotes η_y at the location of the BPM i and k_j is the strength of the skew quadrupole j .) This method is quite similar to an orbit correction and straightforward. However, the η_y -measurement is critical: Vertical dispersion is the dependence of vertical orbit on beam momentum and thus is obtained from a series of orbit measurements for different radio frequency settings. With vertical dispersion in the mm-range and $\pm 0.3\%$ momentum variation, the orbit changes by only a few micrometer. Therefore, even if the machine is in thermal equilibrium, drifts may disturb measurements. In order to perform dispersion measurements sufficiently fast, and therefore avoid drifts, new and faster modes of RF-variation have been implemented (up to 240 Hz/s) which allow to perform an η_y -measurement at $\approx 50 \mu\text{m}$ resolution.

The betatron coupling correction is performed after the dispersion correction since the dispersive skew quadrupoles obviously have an effect on the betatron coupling as well. The 24 non-dispersive skew quadrupoles can correct for this effect without having an influence on the already corrected spurious vertical dispersion since they are at locations with $\eta_x = 0$. The

correction is performed by applying the SVD “inverted” (with appropriate weighting factor cut) model based sensitivity tensor $\partial(\partial x_i/\partial c_j)/\partial k_m$ to the measured coupled orbit response matrix. ($\partial x_i/\partial c_j$ is the 146×146 coupled orbit (BPM/Corrector) response matrix and k_m denotes the strength of the skew quadrupole m .) In order to make use of a 2D-SVD procedure, the tensor is actually rearranged as a 24×146^2 matrix. Multiplication of this matrix with the deviations of the measured orbit response matrix with respect to the model response gives a vector of skew quad increments, which are applied with inverted sign. This method was applied iteratively. In case of large initial deviations, an iteration was also done within the model for updating the sensitivity tensor.

3.2 LET (“low emittance tuning”)

In order to reduce the spurious vertical dispersion further one may apply dispersion-free steering techniques which involve manipulations of the orbit: vertical orbit bumps will sample vertical dipole fields in quadrupoles and skew quadrupole fields in sextupoles. This increases the number of “knobs” available for vertical dispersion and betatron coupling suppression.

The LET (low emittance tuning) algorithm [12] uses an extended, double linear system: the vertical system uses a measurement vector composed from vertical orbit and dispersion and the off-diagonal blocks of the orbit response matrix, and a knob vector containing vertical correctors and skew quadrupoles. The horizontal system uses a measurement vector composed from horizontal orbit and dispersion and the diagonal blocks of the response matrix, and a knob vector containing horizontal correctors. Both systems may also include BPM roll errors. The vertical system will provide correction of vertical dispersion and coupling, and the horizontal system will provide correction of linear optics, i.e. beta functions and horizontal dispersion similar to a LOCO-procedure. To evidence how the LET procedure exploits the sextupoles off axis behavior to correct coupling, in Fig. 3 is shown the influence of sextupoles on the matrix $C_{i,1,k}$, that is a projection of the tensor $C_{i,j,k} = \partial(\partial x_i/\partial c_j^v)\partial c_k^v$ (where x_i is the horizontal orbit and c_j^v and c_k^v are vertical corrector kicks) on the corrector $c_{j=1}^v$.

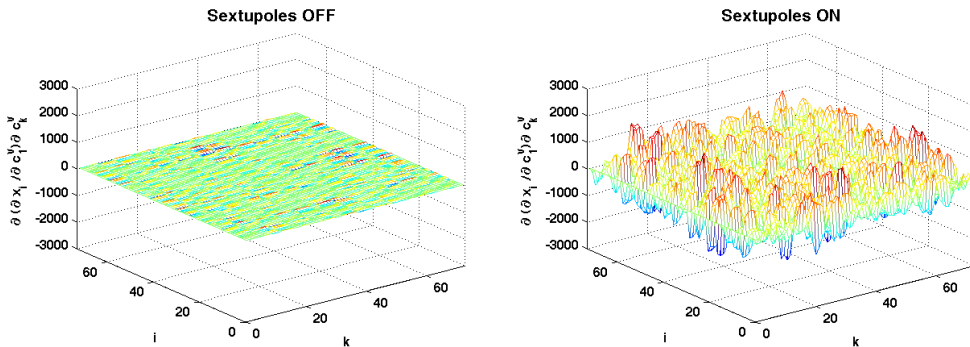


Figure 3: The matrix $C_{i,1,k} = \partial(\partial x_i/\partial c_1^v)\partial c_k^v$ for the horizontal orbit x_i due to the change of vertical correctors c_1^v and c_k^v , with and without sextupoles.

The tensor C is mainly determined by the off axis effect of sextupoles, and thus for vertical orbit excursions (due to c_j^v), by skew quadrupole effects. The tensor $C_{i,j,k}$ rearranged as a matrix of size $(N_i \times N_j) \times N_k$ (where N is the number of monitors or correctors) may be added to the system of equations that determines the correction (c_k^v), enforcing the system to consider the changes of coupling orbit ($\partial x_i / \partial c_j^v$) determined by the presence of sextupoles in the lattice and correcting the coupling effect represented by a non zero $\partial x_i / \partial c_j^v$. The same is true for optics corrections taking the tensor $B_{i,j,k} = \partial(\partial x_i / \partial c_j^h) \partial c_k^h$ (where c_i^h are horizontal corrector kicks). It is also to be noticed that N_j may be less than the total number of correctors (N_k).

Two free parameters shift priority between orbit, dispersion and optics corrections, since the latter two are performed on the expense of orbit excursions in order to sample the down-feeds required. These parameters and the number of SVD weighting factors for solving the systems are chosen at every correction iteration, in order to identify the settings producing the best correction.

LET had been applied successfully to DIAMOND and was compared to LOCO [12]. In 2011/12 it was also applied to the SLS.

4 Model independent correction methods

These methods perform a purely empirical optimization of the machine regardless of the physical model. They just need a set of knobs and a target function which is to be optimized, thus they are related to numerical minimization procedures.

The advantage of these methods is that they avoid problems due to model deficiencies and limited measurement resolution. On the other hand, they are limited by the range and resolution of the target function and they will execute relatively slowly in order to ensure robustness by averaging the target function. Thus they best start on top of a previous model dependent optimization, which has already reached its limit.

One method of this kind has been applied in SVET for coupling suppression:

4.1 RWO (random walk optimization)

For the target function, the measured rms beam height was used, which is obtained from the high resolution π -polarization profile monitor operating in the visible and near UV light region [13]. The vertical emittance then is given from the local beta function. Although the emittance thus obtained is an apparent vertical emittance at one particular location and not necessary equivalent to the equilibrium vertical emittance [14], it had been demonstrated that minimizing the beam height at the monitor also minimizes the equilibrium vertical emittance [13], and, for the well coupling corrected case the apparent emittances around the lattice eventually approach the equilibrium emittance.

The monitor had been specified to resolve beam heights down to about 5 μm rms, which

correspond to 1.8 pm·rad emittance. Extending operation into the 1 pm·rad range ($3.8 \mu\text{m}$ rms) was achieved by additional SRW [15] simulations entered into the monitor's calibration table, and by optimization of some image processing parameters. The lowest beam heights that could be measured were $\approx 3.5 \mu\text{m}$ rms and define the physical limitations of the monitor. Resolving emittances in the sub-pm·rad range will become possible with the new monitor presently under construction.

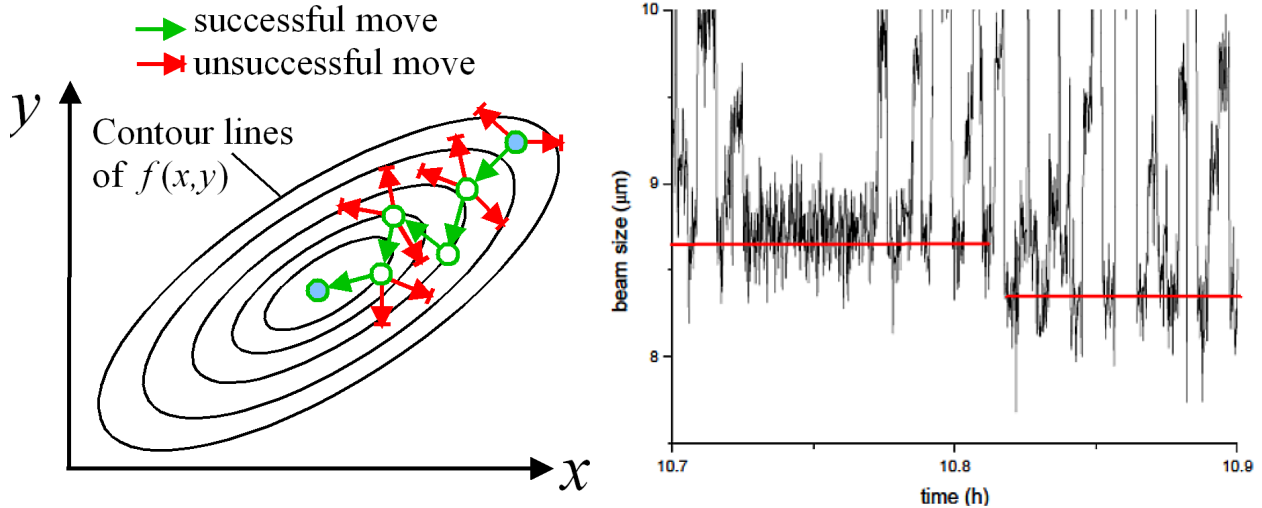


Figure 4: Left: schematics of the RWO searching for a minimum by trial & error. Right: example of a successful move: the fluctuations of the target function (beam size) require averaging.

The 24 non-dispersive skew quadrupoles were chosen as knobs, and the most simple and robust random walk optimization (RWO) method was applied: a random set of skew quad changes is added to the current skew quad settings. If the target function (after some averaging, etc.) shows an improvement, the changes are kept otherwise they are rejected. This is illustrated in Fig. 4, left. This method has the great advantage, that it may run automatically in the background even during user operation, since the step size can be set such that the changes in the vertical beam size are comparable to the fluctuations of the monitor reading (see Fig. 4, right).

5 Implementation

5.1 VRM

The VRM application suite consists of the measurement part which is fully automated in order to guarantee a well defined and fast orbit response matrix and dispersion measurement. Both procedures are implemented as part of the orbit correction facility which gives access to BPM/corrector data and to the online machine model. The response matrix measurement

involves automatic corrector cycling in order to minimize hysteresis effects, a beta function dependent corrector kick determination in order ensure constant orbit amplitudes for safe operation and a corrector kick calibration through comparison of the excited orbit oscillation with the model prediction. The dispersion measurement procedure re-programs the master oscillator for faster frequency variation, determines the necessary frequency changes as a function of beam momentum change, measures difference orbits and performs the dispersion fit. Orbit corrections are applied before and after each step.

The measurement data are then manually submitted to two standalone TRACY-2 based optimizer binaries through plain standardized ASCII files for dispersion and betatron coupling minimization. The optimizers create sequences of EPICS *caput* commands which allow to set the skew quadrupoles according to the prediction.

It is not planned to condense the application suite into one "black box" application, since intermediate results require expert evaluation and parameter adaption for the next steps. Instead it is planned to speed up especially the response matrix measurement which at present takes ~ 15 minutes per plane, since it is carried out by a high level Tcl/Tk script on a console. By pushing the procedure to the middle layer level implementing it in C++ on a server the measurement time and thus the dominating systematic errors originating from drifts can be significantly reduced.

5.2 LET

The LET procedure is implemented in a MATLAB tool with a user interface, shown in Fig. 5. The interface allows the user to select the weight factors and number of eigenvalues to use in the correction, visualize the data and the foreseen correction, acquire data and set the corrector strengths. The data Inupt/Output is performed with the EPICS commands *caget* and *caput*. From the tool it is also possible to evaluate the response matrices used by the correction algorithm using a parallel routine that preforms the evaluation using MADX.

Typically the time needed for a correction iteration is 20 minutes considering 5 to 10 minutes to acquire the data and the same amount of time to determine the wished weight factors.

5.3 RWO

Two small RWO applications with manual and automatic evaluation have been prepared and used in the beam studies. It is necessary to average the target function for several seconds in the automated application to evaluate robustly whether a step is successful or not. Most of the unsuccessful steps, however, can be recognized much faster by eye, i.e. human intelligence, thus a manual optimization can be more efficient.

The step size, the set of correction variables, the distribution of random numbers and the time for averaging can be set up through a GUI. These implementations of RWO required only little efforts: the main routine is realized by less than 100 lines of code.

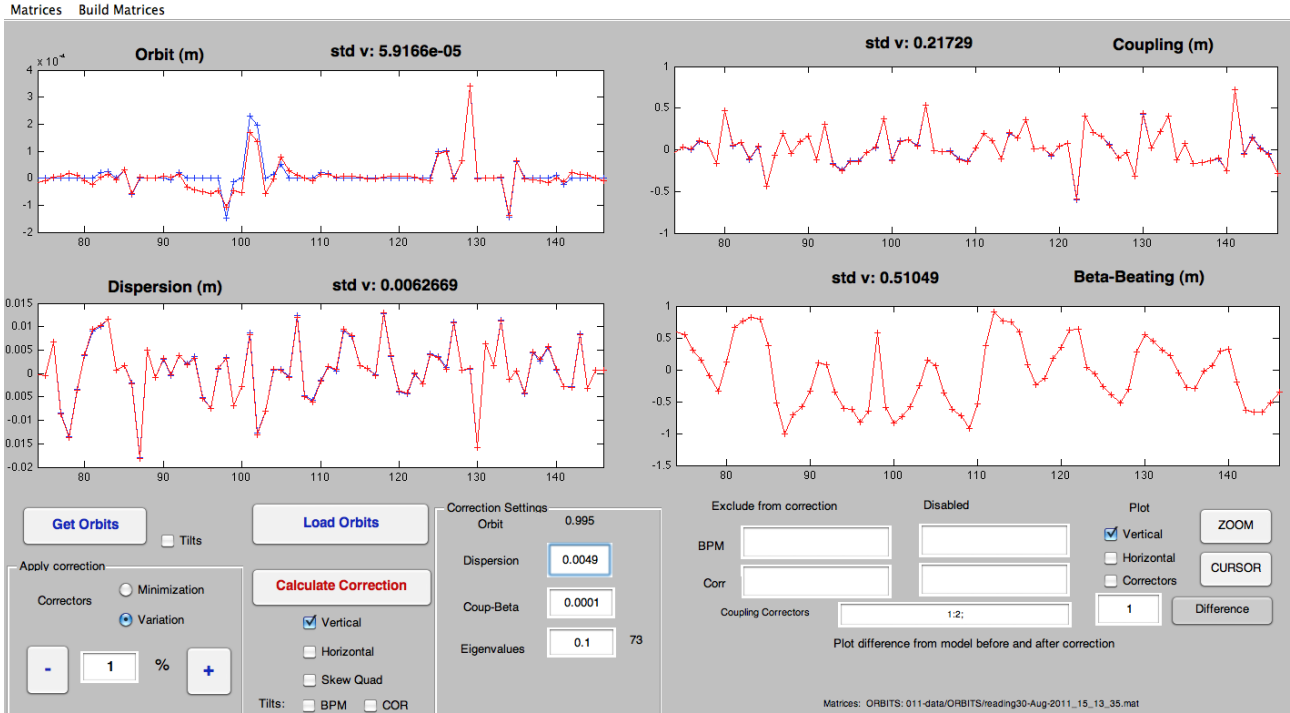


Figure 5: LET Matlab GUI user Interface

6 Results and discussion

Work is going on, so the results reported here are a snapshot of the current status and should not be taken as a comparison of the performance of the different methods, since the results achieved with a particular method depend much on the machine development time spent on its application.

6.1 VRM

VRM has been applied and continuously refined since several years, in its simplest form since the commissioning of the SLS. In parallel, the number of skew quadrupoles was increased in steps from initial 6 to 36, the problem of BPM roll errors was resolved, which had spoiled vertical dispersion measurements, and the BAGA was performed in steps while repairing defective girder movers. Thus the achievements on vertical emittance depend on different measures taken and therefore are not obvious to compare. The best result obtained until now resulted in 1.2 pm-rad of vertical emittance based on a measurement of vertical dispersion with $65 \mu\text{m}$ resolution and suppression to 1.3 mm rms.

6.2 LET

LET has been applied in only 3 MD-shifts up to now. Nevertheless, a vertical emittance of 1.6 pm-rad was achieved already at the expense of an orbit excursion of 30 μm rms.

The first shift has been devoted to the realization and test of the Input/Output, the second has been used to test the vertical correction and the third shift realized an equivalent of the VRM using skew quadrupoles and started to test LET correction with vertical correctors and simultaneous BPM roll estimation [16]:

6.2.1 MD Aug.30, 2011: LET Vertical correction

Orbit, dispersion and coupling orbit before and after LET correction during the second shift are shown in Fig. 6. Three LET correction iterations are performed using only vertical correctors and weights set to correct 94% orbit, 5% dispersion and 1% coupling.

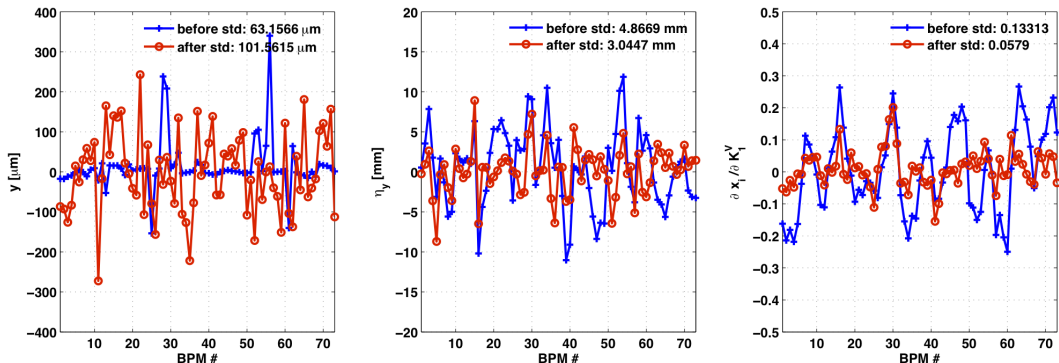


Figure 6: Orbit, dispersion and coupling before and after 3 iterations of LET using vertical correctors measured during the second SLS MD shift (Aug.30, 2011). Vertical beam size before correction $\sigma_y = 16 \mu\text{m}$, after correction $\sigma_y = 7 \mu\text{m}$

The residual orbit observed is 100 μm while the rms dispersion and coupling have been reduced respectively to $\sim 63\%$ and $\sim 44\%$ of their original values. The original vertical beam size of $\sigma_y = 16 \mu\text{m}$, was reduced after correction to $\sigma_y = 7 \mu\text{m}$.

6.2.2 MD Mar.13, 2012: LET Skew quadrupoles, Vertical correction and BPM roll errors

The correction performed with skew quadrupoles within the LET tool is basically identical to the VRM correction, the only differences are the use of a smaller set of correctors in the evaluation of the off diagonal response matrix and the use of a 1D-SVD algorithm to simultaneously constraint dispersion and coupling. In the third shift the correction with skew quadrupoles has

been tested and vertical beam sizes slightly worse (with respect to the ones obtained by VRM) have been measured. Fig. 7 shows the beam size history for this last shift.

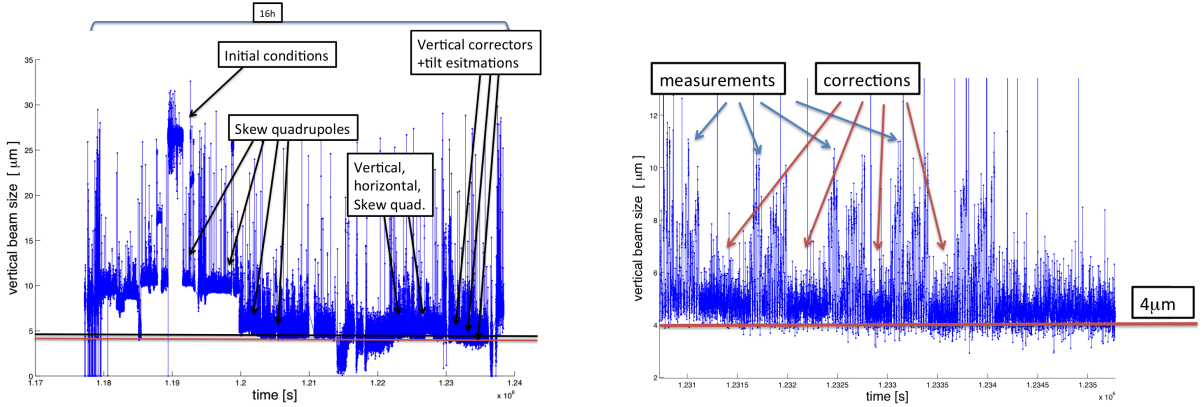


Figure 7: Beam size history during the third LET MD shift: Full history (left), vertical correctors and roll estimation after skew quadrupole corrections (right).

After eight iterations of skew quadrupole correction (alternating dispersive and non dispersive skew quadrupoles), constraining dispersion and the first 15 columns of the off diagonal response matrix, the vertical beam size was reduced to an average beam size of $4.7 \pm 0.2(\text{stat}) \pm 0.5(\text{syst}) \mu\text{m}$. The correction has been performed with 80% weight on dispersion and the residual to correct the off diagonal elements of the response matrix. The eigenvalue cut was set at 10% of the the largest eigenvalue of the SVD decomposition.

Various tests have been performed trying to improve this result, using horizontal correctors, vertical correctors and simultaneous correction with skew quadrupoles and vertical correctors, but none of this could improve the previous minimum vertical beam size. However evaluating vertical corrector strengths including possible monitor roll errors, gave an improvement in the correction. The evaluated roll errors have not been set to correct the measured orbits, but only considered in the evaluation of the corrector strengths, by setting a common roll factor at every beam position monitor for all the measurement taken (the orbit, two off energy orbits for the dispersion measurement and 15×2 orbits with a corrector excited).

The four iterations performed with this extra condition, constraining orbit at 80%, dispersion at 10% and coupling at 10%, using all the available eigenvalues, reduced the vertical beam size to $4.4 \pm 0.4(\text{stat}) \pm 0.5(\text{syst}) \mu\text{m}$. Unfortunately, the beam size measurement was quite noisy, probably due to a coupled bunch instability which disappeared later, and required filtering of the data. The measurement and correction iterations for this set of corrections are shown in more detail in Fig. 7, right. Fig. 8 depicts the change in vertical orbit, dispersion and vertical orbit due to the an horizontal corrector, before and after the various corrections in the last MD-shift.

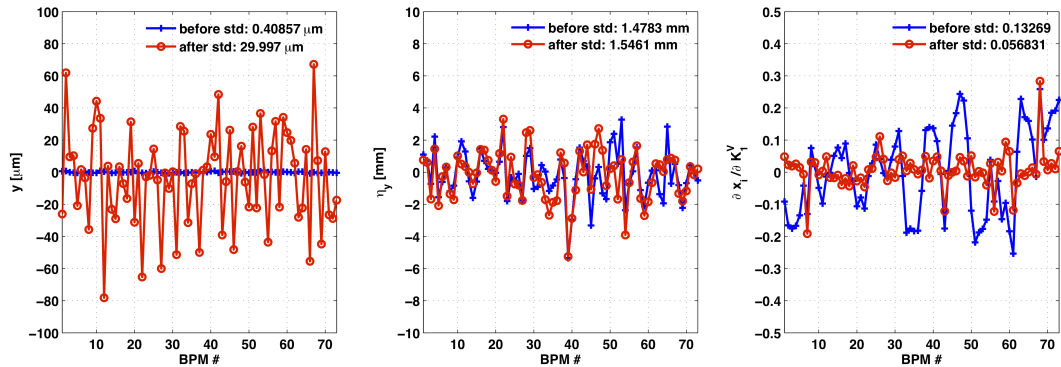


Figure 8: Residual orbit , dispersion and coupling at the beginning of the 3rd shift (Mar.13, 2012) and at the end, after correction with skew quadrupoles, followed by vertical correction and roll estimations. The beam size is $26 \pm 1 \mu\text{m}$ at the beginning of the shift (skew quad set to zero) and $4.4 \pm 0.4(\text{stat}) \pm 0.5(\text{syst}) \mu\text{m}$ at the end of the shift.

6.3 RWO

RWO on top of VRM delivered the world's best value of vertical emittance up to now in the MD-shift at Dec.6, 2011: Fig. 9 shows the evolution of measured beam height. Three iterations of VRM (dispersion and coupling correction) were performed, resulting in a beam size of $4.2 \mu\text{m}$, resp. an emittance of $1.3 \text{ pm}\cdot\text{rad}$. Between the second and third iteration, the emittance monitor was tuned by extending the calibration curve and adjusting image processing parameters. Finally, the RWO was activated and managed to reduce the beam size to $3.6 \pm 0.6 \mu\text{m}$, resp. the emittance to $0.9 \pm 0.4 \text{ pm}\cdot\text{rad}$. The emittance error was derived from error estimates on beam size determination and vertical beta function at the location of the monitor. A measurement of vertical dispersion at the monitor was not done, so there could be some contribution from the beam energy spread to the beam size, and the emittance may be even smaller. At this level, the emittance monitor finally met its lower range of operation, so the RWO's target function saturated and no further optimization was possible.

A response matrix was recorded before and after RWO, confirming a reduction in the rms of the off-diagonal elements which corresponds to a global reduction of betatron coupling, although the vertical beam size was measured only at the location of the monitor. It turned out, that the changes in rms skew quadrupole strength due to RWO were significantly larger (a factor of 6) than expected from the last iteration of systematic correction, indicating that the systematic correction was limited by model deficiencies rather than by pure response matrix measurement errors.

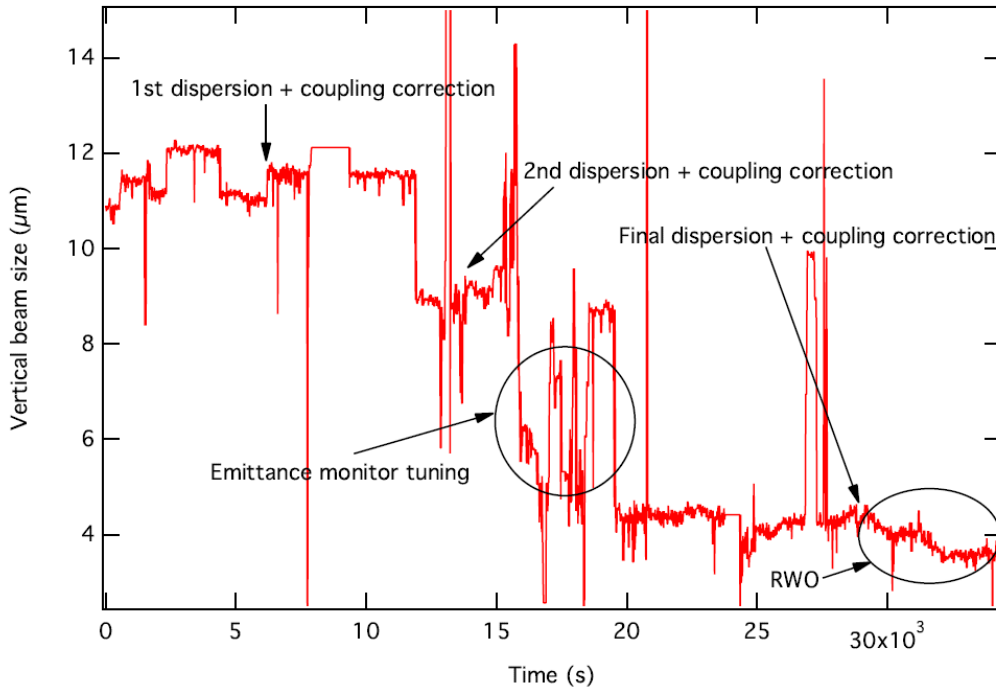


Figure 9: Evolution of vertical beam size (rms) during the machine shift on Dec.6, 2011.

7 Summary and outlook

Methods for vertical emittance tuning have been established:

- BAGA (beam assisted girder alignment) removes steps between girders based on survey data and thus eliminates sources of vertical dispersion. BAGA is only possible due to the SLS dynamic alignment system allowing remote girder moves with stored beam. Regular checks of the mover systems are required.
- VRM (vertical dispersion and coupled response matrix measurement) is a well established method. The measurement is partially automated. Vertical dispersion and betatron coupling are corrected alternating and iterating. Once the machine has reached its thermal equilibrium, results are well reproducible.
- LET (low emittance tuning) performs an integrated correction of the complete response matrix and orbit and optics in both planes, and is also able to determine BPM roll error. It has not been tested much yet at SLS, but the early results are already very promising. More MD-shifts are required.
- RWO (random walk optimization) overcomes model deficiencies and BPM noise by direct trial & error minimization of vertical emittance measured at the monitor and thus is able to push further results obtained with VRM and LET. The performance is presently limited by the resolution of the beam size monitor.

The complete BAGA recently performed (fall 2011) removed misalignments which were present in the storage ring from the very beginning. Also orbit bumps for beam lines could be reduced. This needed to be done only once. The SLS site is rather quiet, settlements are slow and small. So executing BAGA every 1 or 2 years in future seems sufficient

The combination of BAGA, VRM and RWO succeeded in the world record low vertical emittance of 0.9 ± 0.4 pm·rad [17]. LET on top or instead of VRM could lead to even lower values and should be explored further, however for compatibility with synchrotron light users orbit manipulations should be confined to the storage ring arcs in order to not move the photon source points in the straights [18]. RWO basically, given enough time, goes beyond the model and may eventually find the true minimum the machine is physically able to deliver.

However, presently vertical emittance minimization is limited by the resolution of the existing beam size monitor. Construction of the new monitor is in progress at PSI. It should be able to resolve vertical emittances down to ≈ 0.5 pm·rad. Installation is scheduled for the winter 2012/13 shutdown [2], and commissioning should be finished in spring 2013 and will enable further minimization. Design specifications will be subject of our next report TIARA/WP6:SVET D_SPEC.

A coupling feed-back, as it is operational at the ESRF [14], has not yet been fully implemented at SLS. Feed-forwards for insertion devices are partially operational. The RWO, however, basically includes a kind of feed-back, since after a distortion of the machine leading to increased vertical emittance, it would automatically “crawl” back to lower values [19]. As long as distortions are small, RWO may continuously work in the background.

A true emittance knob, i.e. a knob to select some value of vertical emittance, has not been implemented. Anyway, in the context of TIARA/SVET, we are interested in the lowest possible value only. However, for the synchrotron users increasing vertical emittance in a clean way, i.e. by exciting a vertical dispersion wave [20] while suppressing the betatron coupling, in order to gain lifetime resp. less frequent top-up injections, would be desirable.

References

- [1] M. Böge, V. Schlott, A. Streun, “Interim report on existing beam instrumentation at the Swiss Light Source storage ring”, TIARA-REP-WP6-2011-001.
- [2] N. Milas, A. Streun; Åke Andersson; Y. Papaphilippou, F. Antoniou, “Report on existing hardware limitations and needed up grades of the storage ring of the Swiss Light Source”, TIARA-REP-WP6-2011-004.
- [3] M. Böge, B. Keil, P. Pollet, T. Schilcher and V. Schlott, “Commissioning and Operation of the SLS Fast Orbit Feedback,” EPAC-2004.
- [4] M. Aiba, M. Böge, J. Chrin, N. Milas, T. Schilcher, A. Streun, “Comparison of linear optics correction means at the SLS”, Proc. IPAC-2011.

- [5] M. Böge, M. Aiba, A. Lüdeke, N. Milas, A. Streun, “The Swiss Light Source A Test-Bed For Damping Ring Optimization”, IPAC-2010.
- [6] M. Böge, J. Chrin, A. Lüdeke, A. Streun, “Correction of imperfections in the SLS storage ring”, Proc. PAC-2009.
- [7] M. Böge, A. Lüdeke, A. Streun, Å. Andersson, “Ultra-low vertical emittance at the SLS”, PAC-09.
- [8] M. Böge, M. Aiba, N. Milas, A. Streun; S.M. Liuzzo, “SLS Vertical Emittance Tuning”, IPAC-2011.
- [9] A. Streun et. al, “Sub-picosecond X-ray source FEMTO at SLS”, EPAC-2006.
- [10] S. Zelenika et al. “The SLS storage ring support and alignment systems”, Nucl. Instr. Meth. A 467, 99 (2001).
- [11] L. Tanner, F. Jenni, “Digital control for highest precision accelerator power supplies”, PAC-2001.
- [12] S.M. Liuzzo, M.E. Biagini, P. Raimondi; R. Bartolini, “Tests for low vertical emittance at DIAMOND using LET algorithm”, IPAC-2011.
- [13] Å. Andersson, M. Böge, A. Lüdeke, V. Schlott, A. Streun, “Determination of a small vertical electron beam profile and emittance at the Swiss Light Source”, Nucl. Instr. Meth. A 591, 437 (2008).
- [14] A. Franchi, L. Farvacque, J. Chavanne, F. Ewald, B. Nash, K. Scheidt; R. Tomás, “Vertical emittance reduction and preservation in electron storage rings via resonance driving terms correction”, Phys. Rev. ST Accel. Beams 14, 034002 (2011).
- [15] O. Chubar, P. Elleaume, “Accurate and efficient computation of synchrotron radiation in the near field region”, EPAC-1998.
- [16] S. Liuzzo, M. Biagini, M. Aiba, M. Böge, “Tests of the low emittance tuning techniques at SLS and DAΦNE”, IPAC-2012.
- [17] M. Aiba, M. Böge, N. Milas, A. Streun, “Ultra low vertical emittance at SLS through systematic and random walk optimization”, submitted to Nucl. Instr. Meth. A.
- [18] M. Aiba, R. Calaga, R. Tomás, G. Vanbavinckhove, “Coupling and vertical dispersion correction in the SPS”, IPAC-2010.
- [19] M. Aiba, M. Böge, N. Milas, A. Streun, “Random walk optimization in accelerators – vertical emittance tuning at the SLS”, IPAC-2012.
- [20] C. Steier, D. Robin, A. Wolski; G. Portmann, J. Safranek, “Coupling correction and beam dynamics at ultralow vertical emittance in the ALS”, PAC-2003.